JOURNAL OF AGRICULTURAL AND FOOD CHEMISTRY

Plasma-Enhanced Modification of Xanthan Gum and Its Effect on Rheological Properties

SOUJANYA N. JAMPALA,[†,‡] SORIN MANOLACHE,[‡] SUNDARAM GUNASEKARAN,[†] AND FERENCZ S. DENES*[,†,‡]

Department of Biological Systems Engineering and Center for Plasma-Aided Manufacturing, University of Wisconsin−Madison, Madison, Wisconsin 53706

The structure and rheological properties of xanthan gum (XG) modified in a cold plasma environment were investigated. XG was functionalized in a capacitively coupled 13.56-MHz radio frequency dichlorosilane (DS)-plasma conditions and, consecutively, in situ aminated by ethylenediamine. The surface structure of modified XG was evaluated on the basis of survey and high-resolution ESCA, FTIR, and fluorescence labeling techniques. The types of species generated in DS-plasma were reported using residual gas analysis (RGA). The aqueous solutions of modified XG were cross-linked and cured at room temperature to form stable gels. The dynamic rheological characteristics of virgin XG and functionalized and cross-linked XG were compared. It was found that parameters such as plasma treatment time and concentration of solutions can be optimized to form stable gels of XG. Thus, cold plasma technology is a novel, efficient, and nonenzymatic route to modify XG.

KEYWORDS: xanthan gum; cold plasma; primary amine groups; cross-linking; gel

INTRODUCTION

Xanthan gum (XG), an anionic extracellular heteropolysaccharide produced by the bacterium *Xanthomonas campestris*, has size similar to many other biocompatible polysaccharides. The primary structure (*1*) consists of a cellulosic backbone with a mannosyl−glucuronyl−mannose sequence at the C-3 position of alternate glucosyl residues (**Figure 1**). The mannosyl residues on the side chains are modified by acetylation of the inner mannose and pyruvylation of the outer mannose, depending on the growth conditions and bacterial strains (*2*). Most researchers (*3*, *4*) suggest a right-handed double helical state for the native XG molecule, which is stabilized by intermolecular and intramolecular hydrogen bonds (*5*).

XG has exceptional rheological properties and is used commercially in the food, pharmaceutical, and oil industries. Though it does not form a gel, aqueous solutions of XG are highly viscous. XG is biocompatible with several gel-forming and non-gel-forming macromolecules and can even form a stable gel in conjunction with suitable biopolymer systems. Recently, XG has been explored (*6*−*9*) as a potential polymer to form hydrogels and as an excipient for tablets in modern medicine (*10*). Some of these hydrogels based on XG have been cross-linked using agents such as epichlorohydrin (*6*, *9*). Iseki et al. have reported the viscoelastic properties of XG hydrogels formed by annealing in the sol state followed by subsequent cooling (*8*). In recent years, another polysaccharide, chitosan (*11*) or poly(glucosamine), has been extensively studied for hydrogel applications due to the reactive amine groups in the structures. Mixed hydrogel systems of chitosan and xanthan (*7*) are shown to be efficient systems for enzyme immobilization with high mechanical strength due to increased viscosity of the mixture.

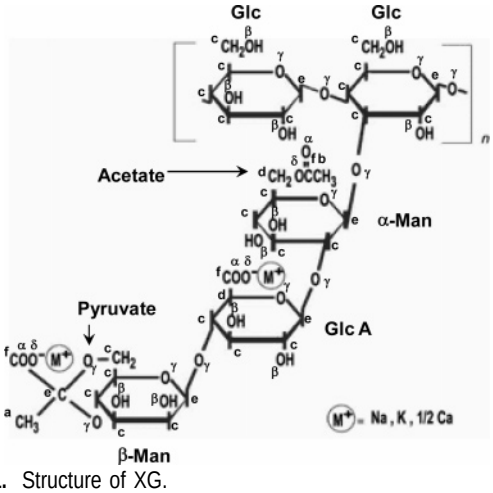

Figure 1. Structure of XG.

Several studies (*12*−*15*) have been reported to engineer the xanthan structure. Various enzymatic (*14*, *15*) and chemical (*13*, *16*) routes to depolymerize and hydrolyze the glucan backbone and the trisaccharide side chain respectively have also been reported. Certain genetic variants of xanthan (*12*) with improved viscometric properties have been synthesized, but little is discussed regarding their physical properties. The reductive amination of XG with sodium cyanoborohydride have very low yield due to the formation of secondary amines (*1*). Behari et al. (*17*) synthesized a copolymer of XG and acrylamide with

* Corresponding author. Telephone: (608) 265-8266. Fax: (608) 262-3632. E-mail: denes@engr.wisc.edu.
† Department of Biological Systems Engineering.
‡ Center for Plasma-Aided Manufacturing.

10.1021/jf0479113 CCC: $30.25
Published on Web 03/31/2005

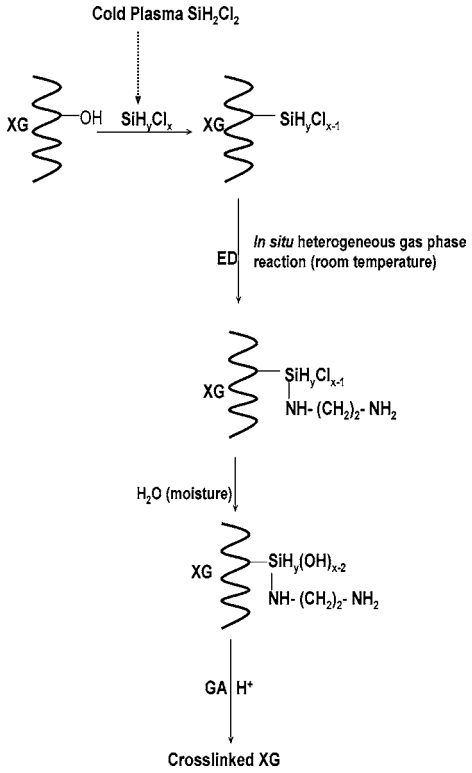

Figure 2. Scheme of modification reaction of XG.

increased thermal stability. Though the chemical, enzymatic, and genetic pathways for xanthan-like polymers have been successfully developed, these methods turn out to be nonselective, tedious, or expensive. If XG can be modified in a controlled manner, several end-use applications can be improved.

Plasma chemical modifications are dry chemistry processes with high energy efficiency and cost-effectiveness. Cold plasma technology is an efficient tool for the incorporation of appropriate functional groups (e.g., amine, carboxyl, hydroxyl) onto various polysaccharides (*18*, *19*). The energy distribution among the plasma species are enough to break the bonds involved in most of the organic molecules and can also lead to the formation of new active chemical states of the carbon atoms (*20*). Thus, organic derivatives can be easily modified under selected discharge parameters through both the gas phase and surface molecular fragmentation and recombination processes. The plasma species penetrate about 100 Å from the surface (*18*) and hence plasma treatment is a surface modification technique.

The rheological and mechanical properties are largely dominated by the chemical nature of the large available specific surface area of the powders, especially whenever they are set in a matrix or dispersion (*21*). As a consequence, plasma-enhanced modification of XG imparts a favorable characteristic to the particle surface.

The objectives of this investigation were (1) to functionalize XG by cold-plasma treatment by grafting primary amine functionalities and by cross-linking using glutaraldehyde and (2) to evaluate the rheological properties of aqueous solutions of the plasma-modified and cross-linked XG.

MATERIALS AND METHODS

Cold-Plasma Modification. Oxygen purchased from Liquid Carbonic Co. was used for the decontamination of the reactor. Dichlorosilane (DS) (97%, bp 8.3 °C), ethylenediamine (ED) (99%, bp 118 °C), glutaraldehyde (GA) (50%), and acetic acid (glacial, 99.99%) were obtained from Aldrich Chemical Co. Fluorescamine used for the identification of primary amine groups was supplied by Molecular Probes Inc. (Eugene, OR). All the chemicals were used without further purification. XG was purchased from Aldrich Chemical Co. and was dried in a vacuum oven at 50 °C for 24 h.

The overall scheme of cross-linking is to implant reactive functionalities such as SiH_xCl_y in a plasma environment, which then are covalently anchored to ethylenediamine under in situ conditions. These primary amine groups at the terminus of modified XG molecule are then cross-linked using glutaraldehyde. A schematic of the procedure is shown in **Figure 2**.

The functionalization and grafting onto XG was performed in a capacitively coupled, rotating glass plasma reactor equipped with a radio frequency (rf) power supply as described previously (*19*). The frequency of rf power used was 13.56 MHz, because this generates less free chlorine and, thus, reduced dehydrochlorination reactions (*22*). The reactor was decontaminated by igniting oxygen plasma (gas pressure, 200 mTorr; rf power, 200 W) for 10 min prior to the plasma treatments on XG. In a typical experiment, vacuum-oven-dried XG powder was introduced into the reactor chamber and a base pressure was established in the chamber and supply lines. The required DS gas pressure was obtained with the aid of flow controllers and corresponding needle valves. The rotation of the reactor was started and the plasma was ignited under the desired experimental conditions and sustained for the given time. At the end of the plasma treatment, the valves were closed and the system was evacuated to the base pressure to purge out the adsorbed gases and byproducts. ED was introduced into the reactor

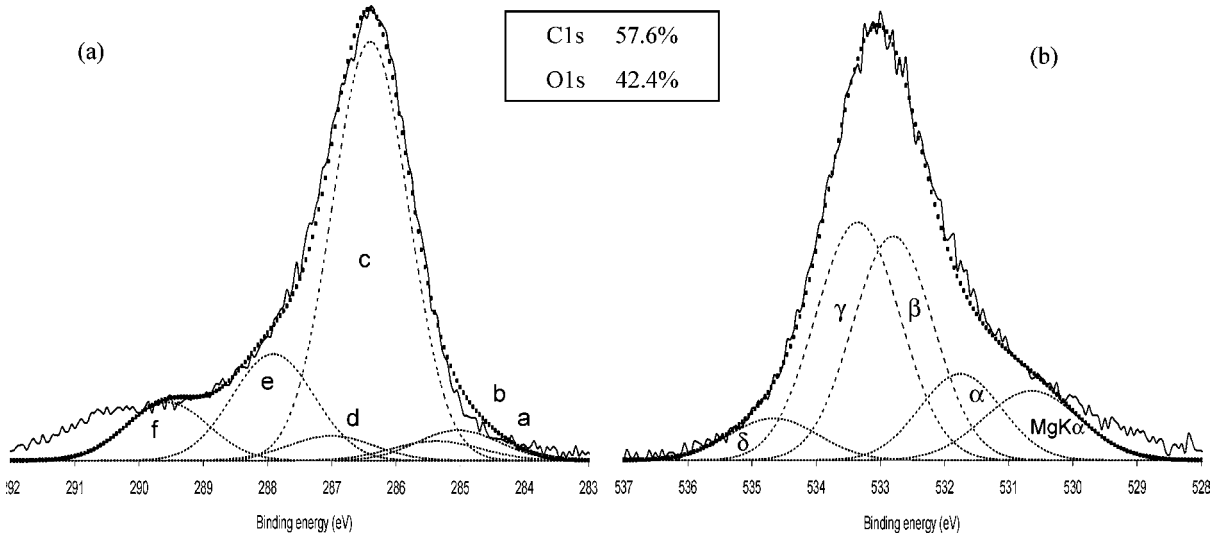

Figure 3. Deconvoluted high-resolution (a) C1s and (b) O1s XPS spectra of virgin XG.

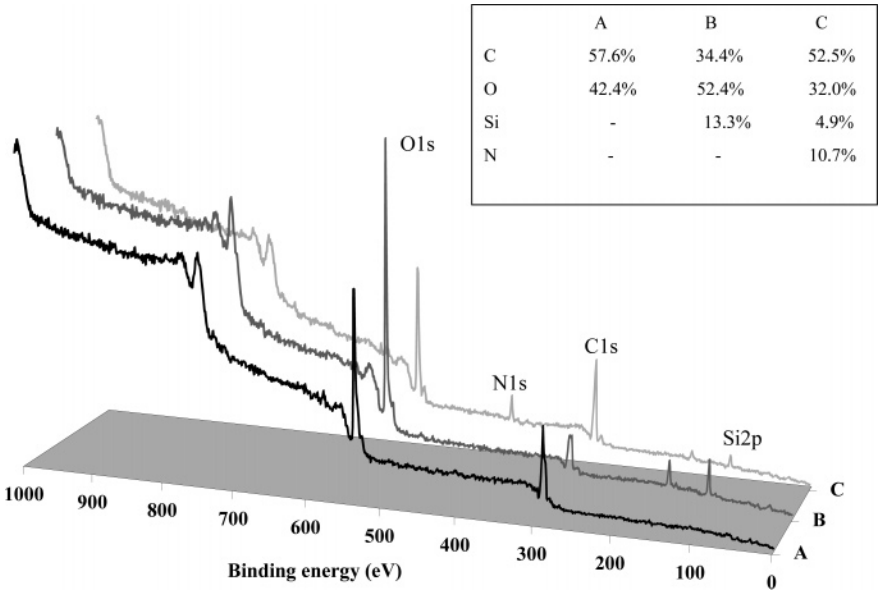

Figure 4. Survey ESCA diagrams of virgin (A), DS-plasma-treated (B), and subsequently in situ ED-grafted (C) XG.

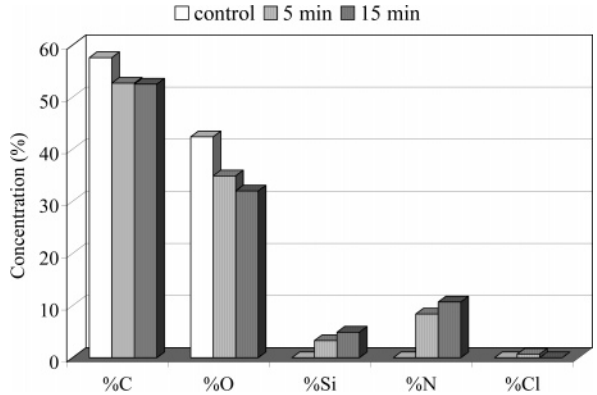

Figure 5. Comparative atomic compositions of virgin, 5- and 15-min DS-plasma-treated, and subsequently grafted XG.

Table 1. High-Resolution XPS Data of Virgin XG

atom	peak	nonequivalent linkage	theoretical composition (%)	BE (eV)	peak area (%)
C1s	a	–*C–C–	2.9	285.0	4.8
	b	–*C–C(O)–	2.9	285.4	3.4
	c	–*C–OH	62.8	286.4	61.7
	d	–O*C–C(O)	5.7	287.0	4.1
	e	–*C═O	17.1	287.9	16.8
	f	–*C(O)–O–	8.6	289.5	9.2
O1s	α	*O═C–O–	10.4	531.8	14.4
	β	H*O–C–	37.9	532.8	37.0
	γ	–C–*O–C–	41.4	533.3	41.0
	δ	–*O–C(O)–	10.3	534.6	7.6

chamber at a pressure of 1000 mTorr for 60 min to complete the grafting reaction. The chamber was evacuated again to remove the unreacted ED. The plasma-functionalized and subsequently aminated XG was removed and stored in a desiccator until further analysis and experiments. The following experimental conditions were used during the plasma treatments: base pressure, 70 mTorr; DS pressure in absence of plasma, 300 mTorr; 13.56-MHz rf power, 100 W; plasma exposure time, 5 or 15 min.

The surface atomic compositions of virgin, plasma-modified, and aminated XG were evaluated using a Perkin-Elmer Physical Electronics 5400 small area ESCA system (Mg source; 15 kV; 300 W; pass energy, 89.45 eV; takeoff angle, 45°). The spectra for carbon (C1s), oxygen (O1s), silicon (Si2p) and nitrogen (N1s) atomic compositions were acquired and their nonequivalent positions in various chemical linkages were analyzed. The surface-charge-origin binding energy (BE) shifts were corrected by references based on well-known C1s peaks (*23*).

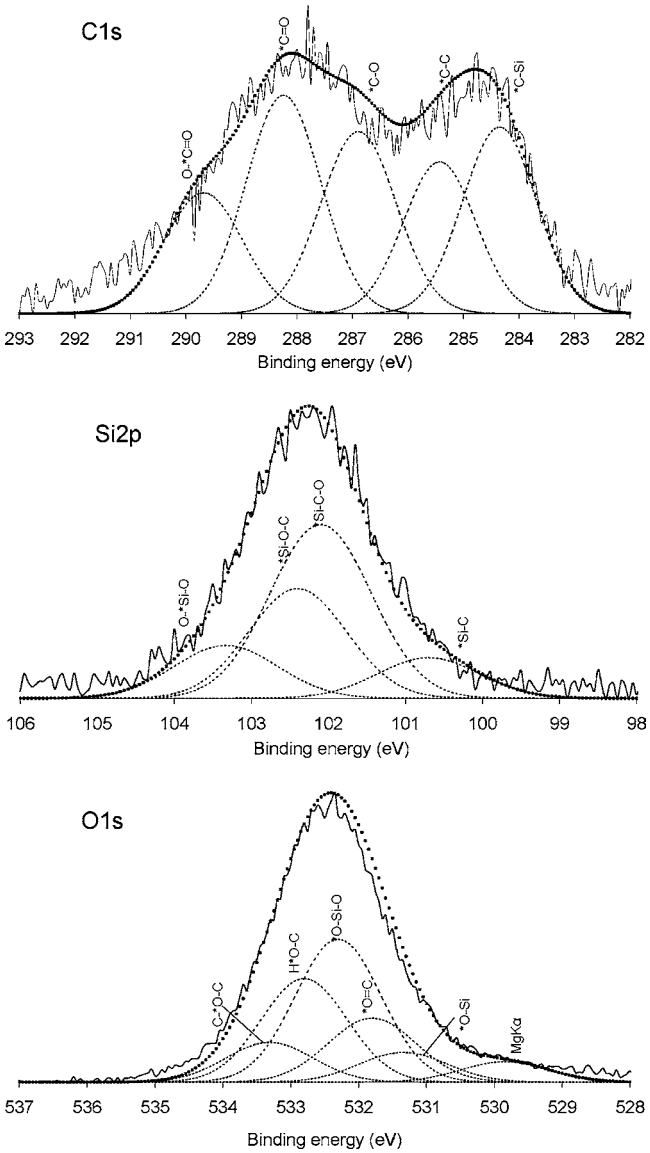

Figure 6. High-resolution ESCA spectra of 15-min DS-plasma-treated XG.

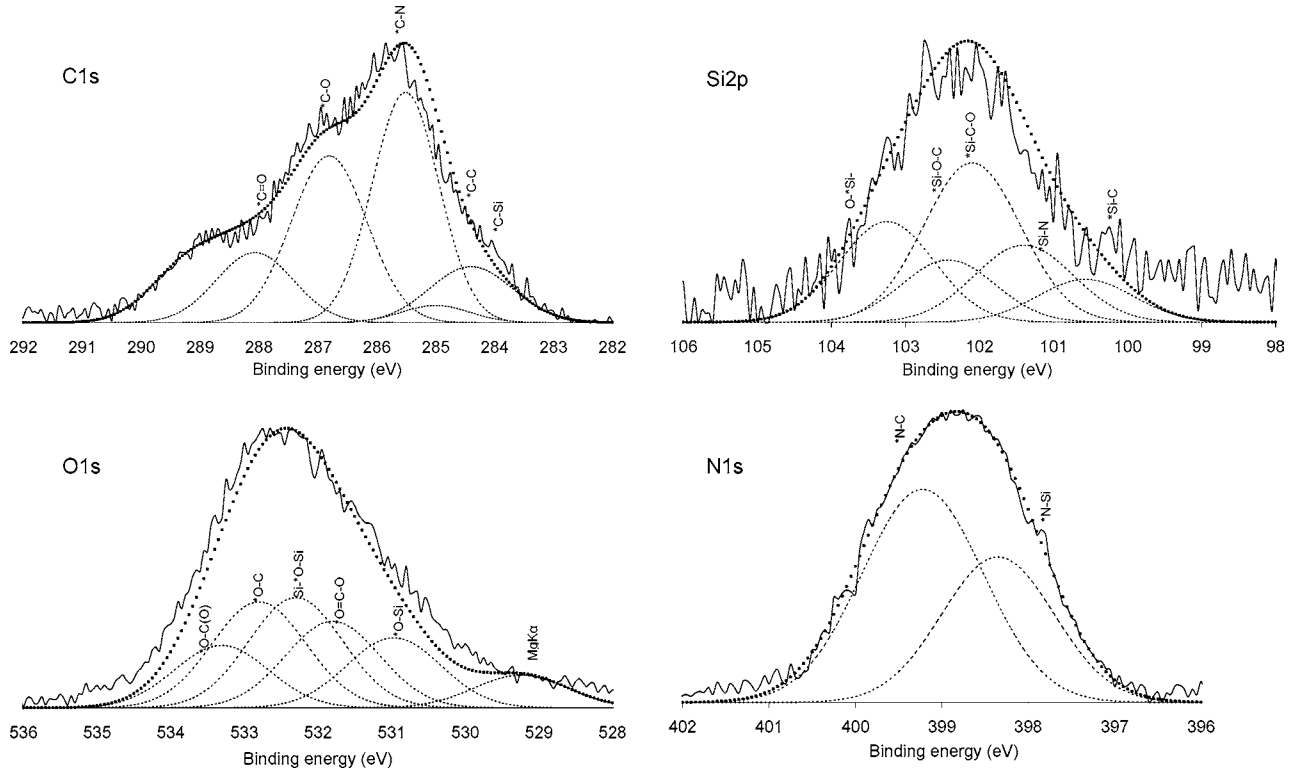

Figure 7. High-resolution ESCA spectra of 15-min DS-plasma-treated and subsequently in situ ED-grafted.

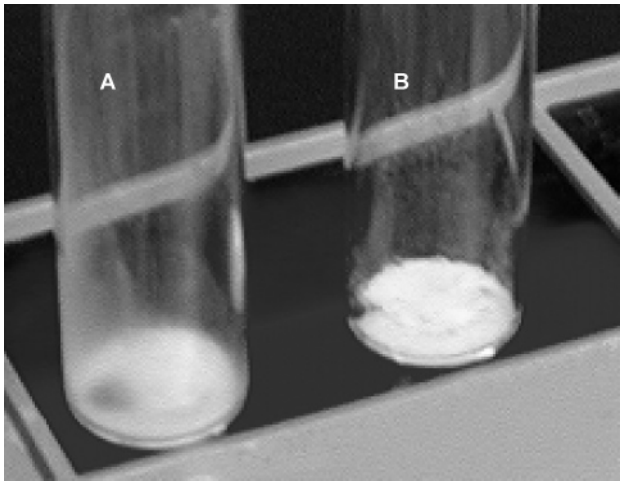

Figure 8. Fluorescamine-labeled (A) virgin XG and (B) plasma-treated and subsequently aminated XG.

Fourier Transform Infrared Spectroscopy (FTIR) was used to identify the chemical linkages on the plasma-functionalized and aminated XG. An ATI-Mattson Research Series IR instrument was used for all measurements. All FTIR evaluations were performed under a nitrogen blanket generated from a flow-controlled liquid nitrogen tank. The dry powder was mixed with KBr (200 mg of KBr and 2 mg of XG) and pressed into pellets using a stainless steel die (International Crystal Laboratories, NJ) and a laboratory press (Fred S. Carver Inc.). Data were collected in the 600−4000 cm^{-1} wavenumber region with 250 scans for each sample, with a resolution of 0.4 cm^{-1}.

The evaluation of primary amine surface functionalities grafted onto XG was done by the fluorescence labeling technique. XG (0.5 g) was placed in a long glass vial and sprayed with fluorescamine solution (0.025% in acetone) using a Gelman Chromist aerosol propellant attached to a polypropylene bottle. The fluorescence of the samples was observed with the aid of a Black-Ray UV lamp (model UBL 21, UVP Inc., San Gabriel, CA) and images were taken with a camera.

A MKS Instruments Spectra Products Residual Gas Analysis (RGA) LM78/LM505 mass spectrometry system was used to identify the various compounds formed from the recombination of molecular fragments during the thermal decomposition of DS. The RGA has 200 Da molecular mass range and sampling was done at the exhaust line of the reactor for the full scan range using a separation valve and a metering valve.

Rheological Evaluations. The aqueous solutions of XG were prepared by slowly dissolving the powder in distilled water. XG was completely dissolved by mixing on a magnetic stirrer for another 30 min at room temperature. The pH of the solutions was adjusted to 5.5 using 1 N acetic acid. GA was added at a concentration of 2% and the solutions were mixed on the magnetic stirrer for additional 30 min. The samples were then cured at room temperature for 8 h. Viscoelastic measurements of virgin and plasma functionalized and subsequently aminated XG were carried out in a controlled-stress dynamic rheometer (Bohlin CVOR, Bohlin Instruments Inc.) using a parallel plate geometry of 20 mm diameter. All the samples were covered with a thin layer of paraffin oil to prevent evaporation of water during the experiments. The duplicate rheological measurements were done to ensure that there was no interaction with the paraffin oil. Dynamic frequency sweeps were performed at isothermal condition of 50 °C with a frequency range from 0.001 to 10 Hz at constant strain amplitude of 1% to ensure the linear viscoelastic region. Temperature sweep was done at a constant frequency of 0.1 Hz and maximum target strain of 1% in the temperature range from 60 to 10 °C with the cooling rate of 1 °C/min. The storage modulus (G') and loss modulus (G'') data were recorded.

RESULTS AND DISCUSSION

Cold Plasma Modification. Figure 3 shows the high-resolution C1s (a) and O1s (b) spectra for virgin XG. The peaks obtained by Gaussian fitting indicate five different types of carbon linkages and four different types of oxygen linkages. A detailed analysis of the various chemical linkages and the corresponding peak ratios are represented in **Figures 1** and **3** and **Table 1**. Both BE values and the peak area ratios of atoms in nonequivalent linkages of virgin XG are in good agreement with the chemical structure of XG (**Figure 1**). All the BE assignments are done using the database for polymeric compounds (*23*).

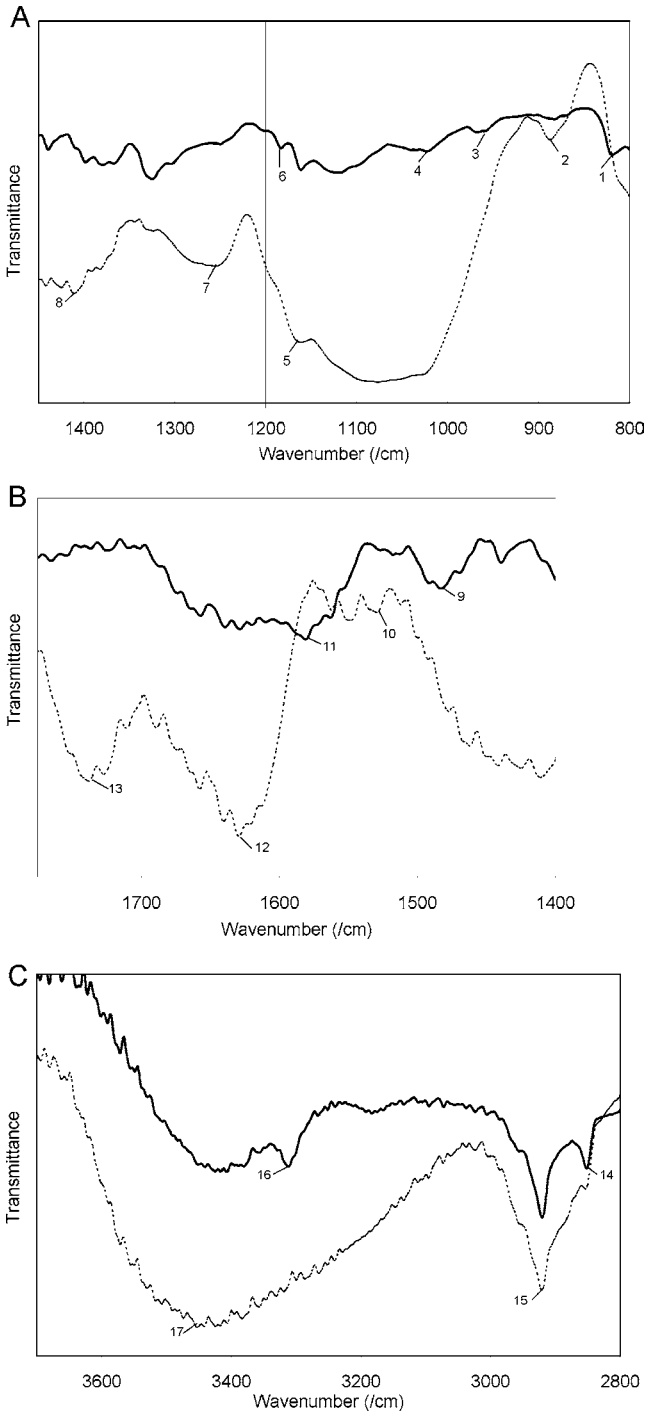

Figure 9. FTIR spectra of virgin XG (--) and plasma-treated and aminated XG (–).

The typical ESCA survey diagrams of virgin (A), DS-plasma-treated (B), and subsequently in situ ED-grafted (C) XG are shown in **Figure 4**. The higher oxygen content and absence of any Cl2p peak in DS-plasma-treated XG can be attributed to the postplasma hydrolysis of SiH_xCl_y groups generated in the plasma environment. After the in situ grafting reaction with ED, the oxygen content decreased, suggesting that some of the free radical sites covalently reacted with ED. The presence of N1s in ED-grafted XG confirms that ED has been successfully grafted onto plasma-treated XG. As per the chemical structure of ED, there are two N atoms per ED molecule and the N/Si atomic ratio obtained from ESCA is around 2.2. Hence, it can be concluded that most of the ED is grafted onto XG through the Si-containing plasma-created functionalities (SiH_xCl_y).

Table 2. Transmittance Band Assignments for FTIR Spectra

peak no.	wavenumber (cm^{-1})	functional group assignment
1	822	Si–N stretch
2	890	C–H of β-pyranose
3	958	Si–N stretch
4	1026	Si–O–Si, C–O–Si
5	1166	–C–O–C– acetal
6	1186	NH wag–rock
7	1257	–C–O–C–
8	1413	–COO–
9	1483	CH_2 bending
10	1530	–COO–
11	1581	$–NH_2$, NH bend
12	1629	–C═O of pyruvate
13	1739	–C═O of acid anhydride
14	2852	CH
15	2921	$–CH_2$
16	3315	$–NH_2$, NH stretch
17	3455	–OH

The atomic compositions of virgin, 5- and 15-min DS-plasma-treated, and subsequently aminated XG are compared in **Figure 5**. It can be observed that even 5 min of plasma treatment is sufficient for the grafting of functional groups, with the concentration of N equal to 8.7%. Small quantities of Cl (0.7%) are found on the 5-min sample, though this peak disappeared in XG treated for 15 min.

The high-resolution ESCA spectra for C1s, Si2p, O1s, and N1s of DS-plasma-treated and ED-grafted XG with possible peak assignments are presented in **Figures 6** and **7**. In addition to the characteristic peaks in deconvoluted C1s in virgin XG, there are C−Si (284.4 eV) and C−N (285.6 eV) peaks present in plasma-treated and aminated XG. It should be noted that the BE values of C−OH, C−O−C, and C−O−Si are close enough to fit under one peak at 286.8 eV. The peak area ratios of C−O/O−C−O (0.8) and C−O/O═C−O (1.5) in plasma-treated XG are significantly reduced from the ratios in virgin XG (C−O/O−C−O, 3.9; C−O/O═C−O, 7.15). This suggests that functionalities similar to O−C−O−Si and O═C−O−Si are present with identical BE values. With this, the argument that most of the implantation of SiH_xCl_y groups takes place at C−O linkages and not C−C linkages is strengthened. The Si2p high-resolution ESCA spectrum for plasma-treated XG exhibits a quadramodal pattern with assigned peaks (*24*, *25*) at 100.7, 102.1, 102.4, and 103.3 eV for Si−C, Si−C−O, Si−O−C, and O−Si−O linkages, respectively. The high surface areas of oxygen related functionalities confirm that the plasma-generated species connect mainly through bonds with oxygen and not with carbon. Also, some of these functionalities are a result of hydrolysis of SiH_x-Cl_y groups under open laboratory conditions. An additional peak for Si−N at 101.4 eV was identified in ED-grafted XG. The bimodal pattern of N1s nonequivalent high-resolution ESCA spectrum of modified XG is fitted with linkages of type Si−N (398.4 eV) and C−N (399.4 eV). The O1s spectra of both plasma-treated and aminated XG are deconvoluted with two new peaks for O−Si (531.3 eV) and O−Si−O (532.3 eV) in addition to peaks with identical BE values as mentioned for virgin XG.

The presence of primary amine groups on plasma-treated and subsequently ED-grafted XG is verified by labeling the samples with fluorescamine. Intense brightness in plasma-modified XG (**Figure 8**) confirms the presence of primary amine groups. No fluorescence was observed in virgin XG.

Figure 9A−C shows the differential FTIR spectra of aminated XG obtained from subtracting the spectrum of virgin XG. For comparison, IR spectrum of XG is plotted in the same figure. The respective peak assignments are summarized in **Table 2**. The characteristic absorptions in XG are well-known (*26*) and

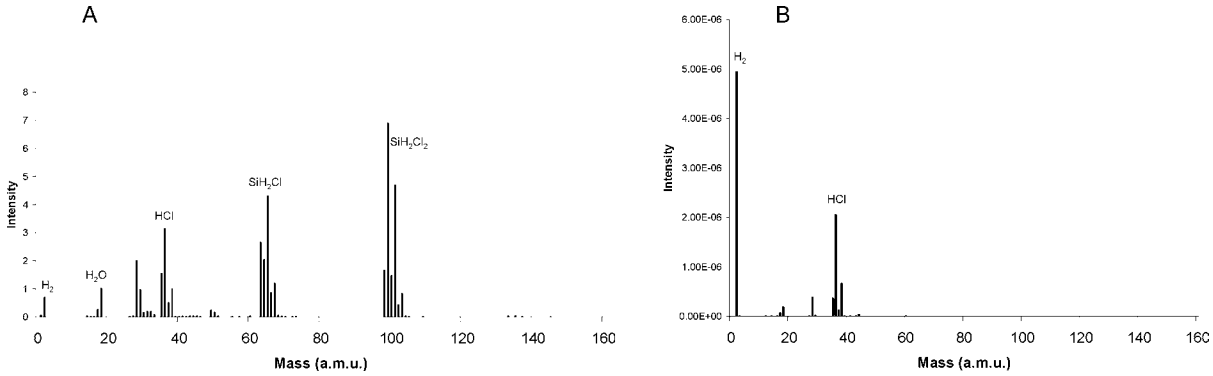

Figure 10. RGA mass spectra of (A) DS in the absence of plasma and (B) DS-plasma (250 mTorr, 100 W) in the presence of samples in reactor.

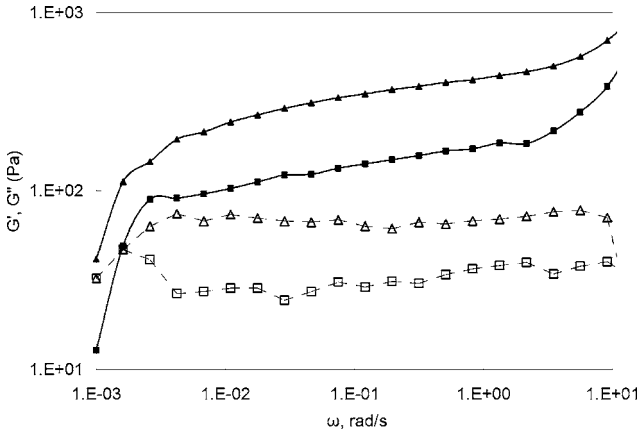

Figure 11. Frequency dependence of elastic (*G′*, filled symbols) and viscous (*G″*, open symbols) moduli of 2 wt % virgin XG (-■-) and cross-linked XG-P5 (-▲-) at $T = 50$ °C and $\gamma = 1\%$.

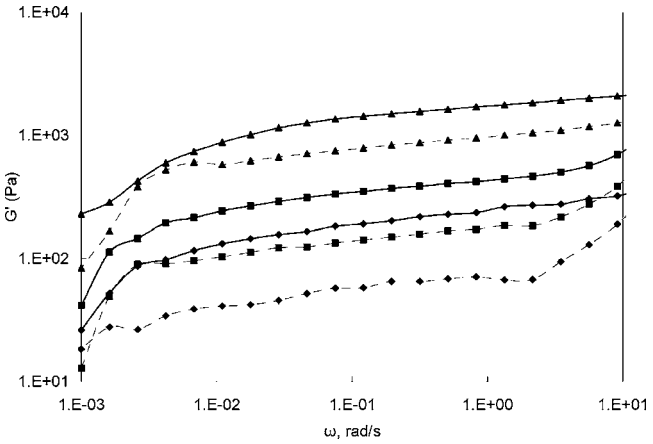

Figure 12. Elastic modulus (*G′*) of virgin (---) and cross-linked XG-5 (–) at 1.75 wt % (-◆-), 2 wt % (-■-), and 4 wt % (-▲-).

all are found in the virgin XG we used. The plasma-functionalized XG exhibits intense bands in the 800−1450 cm^{-1} region, including stretching of Si−N (*27*) and vibrations due to Si−O−Si and C−O−Si (*28*). The presence of bands around 1186, 1581, and 3315 cm^{-1} confirms that the primary amine groups have been successfully grafted due to plasma treatment and subsequent in situ reaction with ED.

RGA spectra (**Figure 10**) recorded before and after ignition of plasma prove the high reactivity of the DS-plasma. Mass spectra of the exhaust gas before plasma ignition (**Figure 10A**) shows the presence of SiH_2Cl_2 (ions' group at 99 Da) and fragments generated in the mass spectrometer ionization chamber, $-SiH_2Cl$ (ions' group at 65 Da), HCl (ions' group at 36 Da), and Si (28 Da). The presence of chlorine with 35 and 36 Da isotopes generates the specific halogen pattern in the ion groups of SiH_2Cl_2, SiH_2Cl, and HCl. After ignition and stabilization of the plasma (**Figure 10B**), only HCl and water signals remain in the RGA-recorded mass spectra. This proves that the plasma is breaking down DS to very reactive radicals that react with the XG substrate at high yields. It can be noted that the main volatile products of the plasma reaction are hydrochloric acid and hydrogen; just small amount of silane remained in the exhaust byproducts.

Rheological Evaluations. Rheological measurements were done on XG that was 5-min (XG-5) DS-plasma treated (gas pressure, 300 mTorr; rf power, 100 W) and in situ reacted with ED. The representative frequency sweeps for a 2 wt % solution of virgin XG and cross-linked and cured XG-5 are presented in **Figure 11**. Both virgin XG and XG-5 form soft gels, as indicated by the dominance of the elastic modulus G′ over the viscous modulus *G″* (*29*). The dynamic moduli of XG-5 lie above that of virgin XG over the frequency range from 10^{-3} to 10^{1} Hz. This suggests that the network strength of XG increases due to the plasma-induced modification and subsequent amination reaction. However, the frequency dependence of *G′* indicates that a stable gel is not formed with the 2 wt % solution of plasma-modified XG. The frequency spectrum at various concentrations of 1.75, 2, and 4 wt % are presented in **Figure 12**. The difference in *G′* between virgin XG and cross-linked XG-5 decreases with concentration. This can be attributed to the increased junction points and entanglements at higher concentrations, which in turn suppress the effect of the cross-linking with GA. Thus, a stable gel cannot be obtained by just increasing the solution concentration.

The degree of frequency (ω) dependence of *G′* can be quantitatively described by a relationship proposed (*30*) by Egelandsdal et al.

$$\log G' = n \log \omega + k \qquad (1)$$

where *k* and *n* are constants. The constant *n* is the slope of the log−log plot of *G′* versus ω. For a physical gel, $n > 0$, and for a chemical gel, $n = 0$. Thus, the *n* value can be used as a measure of the resemblance of a gel to a chemical gel. Such a plot (**Figure 13**) yielded an *n* value of 0.2 for cross-linked XG-5 at various concentrations. Thus, these systems do not form a stable gel and exhibit a creeping behavior. The temperature sweep data are presented in **Figure 14**. In this plot we observe a *G′*−*G″* crossover point around 55 °C for 1.75 wt % of XG-5. This is generally considered as the gel point. However, no such crossover point was observed in the temperature range of our study for the 4 wt % XG-5 system.

Similar analyses were done for 15-min plasma-treated and aminated XG (XG-15) at lower concentrations of 0.5 and 1 wt

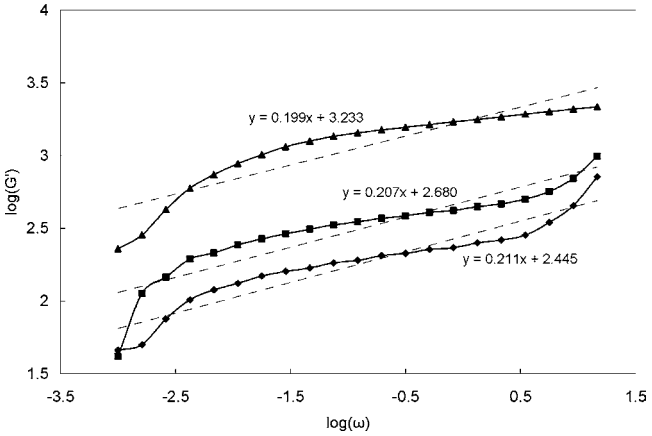

Figure 13. log–log plot of G' vs ω for cross-linked XG-5 at 1.75 wt % (-♦-), 2 wt % (-■-), and 4 wt % (-▲-) concentrations.

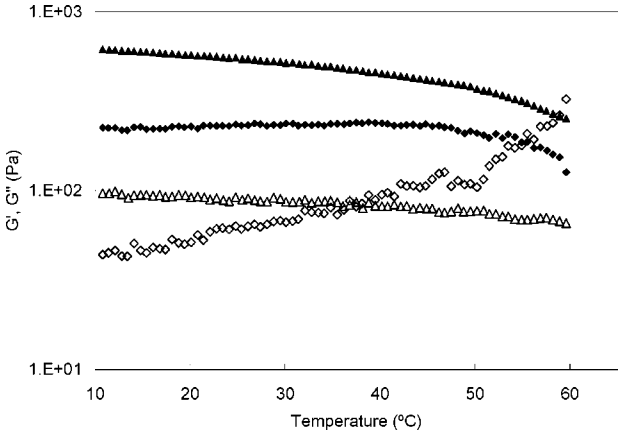

Figure 14. Temperature dependence on G' (filled symbols) and G'' (open symbols) with 1 °C/min cooling rate and $\gamma = 1\%$ on 1.75 wt % (-♦-) and 4 wt % (-▲-) cross-linked XG-5.

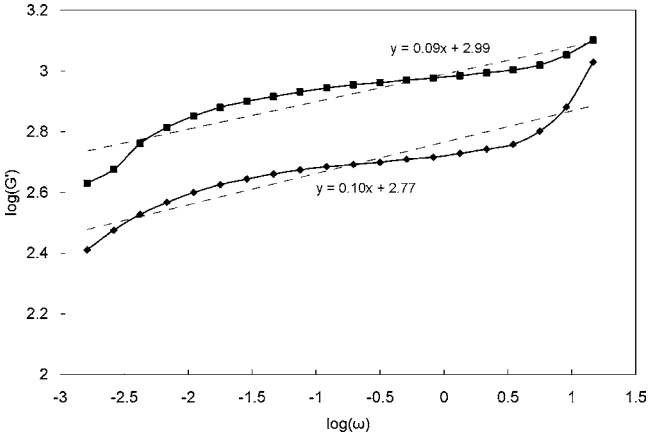

Figure 15. log–log plot of G' vs ω for cross-linked XG-15 at 0.5 wt % (-♦-) and 1 wt % (-■-) concentration.

%. The frequency sweeps data for these systems are shown in **Figure 15**. In this plot, G' is fairly linear over the entire experimental frequency range and is less frequency-dependent than the XG-5 systems (**Figure 12**). It is well-known that a characteristic of G' observed for true gels is frequency-independent (*8*). On close observation, we can see that the gel strength (G') of 1 wt % XG-15 was comparable to that of 4 wt % XG-5. Further, the *n*-value for the XG-15 systems are fairly small ($n \sim 0.1$). This confirms that the duration of plasma treatment plays an important role in the rheological properties

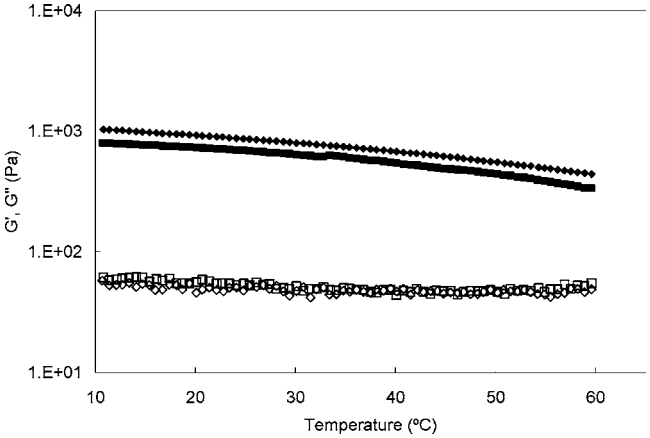

Figure 16. Temperature dependence of G' (filled symbols) and G'' (closed symbols) of 0.5 wt % (-♦-) and 1 wt % (-■-).

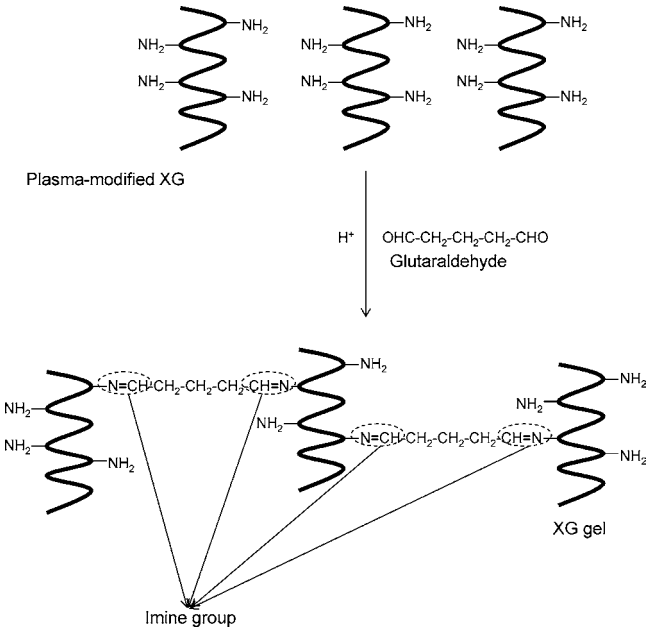

Figure 17. Schematic illustration of the cross-linking mechanism.

of XG solutions, and fairly stable gels may be formed by suitably optimizing the plasma treatment duration and polymer concentration. The temperature sweep spectra for XG-15 systems presented in **Figure 16** do not show a $G'-G''$ crossover point, and this suggests that the gel point may be far above 60 °C.

The suggested glutaraldehyde-activated cross-linking route is illustrated in **Figure 17**. The presence of the primary amine groups on XG polymeric chains after plasma modification and in situ amination ensures their greater activity with dialdehydic glutaraldehyde. In the reaction, aminated XG is derivatized with glutaraldehyde to give formyl coupling sites for reaction with another XG molecule and thus form ionic links. The cross-linked XG polymer network hydrogels are based on physical and chemical cross-links. It is due to the formation of C═N due to imine reaction and interactions between the primary amine group and the aldehyde group, including the hydrogen bonding displaying the equilibrium swelling properties. Imine formation is an acid-catalyzed process with a maximum rate at a weakly acidic pH. It involves nucleophilic attack on the carbonyl group by the lone pair of electrons of the nitrogen atom of the primary amine, resulting in a dipolar intermediate. Proton transfer from nitrogen to oxygen leads to a neutral amino alcohol. The acid

catalyst promotes the protonation of the hydroxyl oxygen, which is a good leaving group. The loss of water produces an iminium ion. The positive charge on nitrogen drives the loss of a proton, giving the final product.

In conclusion, XG has been successfully grafted with reactive SiH_xCl_y functionalities in DS-cold-plasma environment. The subsequent in situ grafting of primary amine groups facilitated cross-linking of XG. The cold-plasma modification improves the network strength, as measured by the dynamic storage modulus, G', of the aqueous solutions of XG. By increasing the plasma treatment time, the frequency independence of the XG network improved, indicating that plasma treatment time and polymer concentration may be optimized to obtain a stable gel from otherwise non-gel-forming XG. Thus, the cold-plasma process proves to be an efficient nonenzymatic route to modify XG such that a stable gel can be formed.

ABBREVIATIONS USED

XG, xanthan gum; DS, dichlorosilane; ED, ethylenediamine; GA, glutaraldehyde; XG-5, 5-min plasma-modified XG; XG-15, 15-min plasma-modified XG.

ACKNOWLEDGMENT

This work was supported in part by a funding from the SC Johnson & Son Inc., Racine, WI.

LITERATURE CITED

(1) Lapasin, R.; Pricl, S. *Rheology of Industrial Polysaccharides: Theory and Applications*; Aspen Publishers: Gaithersburg, MD, 1999.

(2) Stokke, B. T.; Christensen, B. E.; Smidsrød, O. Macromolecular Properties of Xanthan. In *Polysaccharides: Structural Diversity and Functional Versatility*; Dumitriu, S., Ed.; Marcel Dekker: New York, 1998; pp 433−472.

(3) Holzwarth, G.; Prestridge, E. B. Multistranded Helix in Xanthan Polysaccharide. *Science* **1977**, *197*, 757−759.

(4) Camesano, T. A.; Wilkinson, K. J. Single Molecule Study of Xanthan Conformation Using Atomic Force Microscopy. *Biomacromolecules* **2001**, *2*, 1184−1191.

(5) Ogawa, K.; Yui, T. X-ray Diffraction Study of Polysaccharides. In *Polysaccharides: Structural Diversity and Functional Versatility*; Dumitriu, S., Ed.; Marcel Dekker: New York, 1998; pp 101−130.

(6) Dumitriu, S.; Dumitriu, M.; Teaca, G. Bioactive Polymers 65-Studies of cross-linked xanthan hydrogels as supports in drug retardation. *Clin. Mater.* **1990**, *6*, 265−276.

(7) Dumitriu, S.; Chornet, E. Immobilization of Xylanase in Chitosan-Xanthan Hydrogels. *Biotechnol. Prog.* **1997**, *13*, 539−545.

(8) Iseki, T.; Takahashi, M.; Hattori, H.; Hatakeyama, T.; Hatakeyama, H. Viscoelastic properties of xanthan gum hydrogels annealed in the sol state. *Food Hydrocolloids* **2001**, *15*, 503−506.

(9) Alupei, I. C.; Popa, M.; Hamcerencu, M.; Abadie, M. J. M. Superabsorbant hydrogels based on xanthan and poly(vinyl alcohol) 1. The study of the swelling properties. *Eur. Polym. J.* **2002**, *38*, 2313−2320.

(10) Talukdar, M. M.; Mooter, G. V. d.; Augustijns, P.; Tjandra-Maga, T.; Verbeke, N.; Kinget, R. In vivo evaluation of xanthan gum as a potential excipient for oral controlled-release matrix tablet formation. *Int. J. Pharm.* **1998**, *169*, 105−113.

(11) Genta, I.; Costantini, M.; Asti, A.; Conti, B.; Montanari, L. Influence of glutaraldehyde on drug release and mucoadhesive properties of chitosan microspheres. *Carbohydr. Polym.* **1998**, *36*, 81−88.

(12) Hassler, R. A.; Doherty, D. H. Genetic Engineering of Polysaccharide Structure: Production of Variants of Xanthan Gum in *Xanthomonas campestris*. *Biotechnol. Prog.* **1990**, *6*, 182−187.

(13) Christensen, B. E.; Smidsrød, O. Hydrolysis of xanthan in dilute acid: Effects on chemical composition, conformation, and intrinsic viscosity. *Carbohydr. Res.* **1991**, *214*, 55−69.

(14) Nankai, H.; Hashimoto, W.; Miki, H.; Kawai, S.; Murata, K. Microbial System for Polysaccharide Depolymerization: Enzymatic Route for Xanthan Depolymerization by *Bacillus* sp. Strain GL1. *Appl. Environ. Microbiol.* **1999**, *65*, 2520−2526.

(15) Sutherland, I. W. Hydrolysis of Unordered Xanthan in solution by Fungal Cellulases. *Carbohydr. Res.* **1984**, *131*, 93−104.

(16) Christensen, B. E.; Smidsrød, O.; Elgsaeter, A.; Stokke, B. T. Depolymerization of double-stranded xanthan by acid hydrolysis: Characterization of partially degraded double strands and single-stranded oligomers released from the ordered structures. *Macromolecules* **1993**, *26*, 6111−6120.

(17) Behari, K.; Pandey, P. K.; Kumar, R.; Taunk, K. Graft copolymerization of acrylamide onto xanthan gum. *Carbohydr. Polym.* **2001**, *46*, 185−189.

(18) Hua, Z. Q.; Sitaru, R.; Denes, F.; Young, R. A. Mechanisms of Oxygen- and Argon-RF-Plasma-Induced Surface Chemistry of Cellulose. *Plasmas Polym.* **1997**, *2*, 199−224.

(19) Ma, Y. C.; Manolache, S.; Sarmadi, M.; Denes, F. Plasma-enhanced synthesis of maltodextrin−polydimethylsiloxane graft copolymers. *J. Appl. Polym. Sci.* **2001**, *80*, 1120−1129.

(20) Behnisch, J. Plasmachemical modification of natural polymers. In *Plasma Processing of Polymers*; d'Agostino, R., Favia, P., Fracassi, F., Eds.; Kluwer Academic Publishers: Dordrecht, The Netherlands, 1997; pp 345−364.

(21) Ihara, T. Plasma Treatment of Powders. In *Plasma Processing of Polymers*; d'Agostino, R., Favia, P., Fracassi, F., Eds.; Kluwer Academic Publishers: Dordrecht, The Netherlands, 1997; pp 395−410.

(22) Manolache, S.; Sarfaty, M.; Denes, F. RF frequency effects on molecular fragmentation. *Plasma Sources Sci. Technol.* **2000**, *9*, 37−44.

(23) Beamson, G.; Briggs, D. *High-resolution XPS of organic polymers: The Scienta ESCA 300 database*; John Wiley & Sons Ltd.: Chichester, West Sussex, England, 1992.

(24) Inagaki, N.; Kondo, S.; Hirata, M.; Urushibata, H. Plasma Polymerization of Organosilicon Compounds. *J. Appl. Polym. Sci.* **1985**, *30*, 3385−3395.

(25) Fonseca, J. L. C.; Badyal, J. P. S. Plasma Polymerization of Hexamethyldisilane onto Polyethylene Film. *Macromolecules* **1992**, *25*, 4730−4733.

(26) Su, L.; Ji, W. K.; Lan, W. Z.; Dong, X. Q. Chemical modification of xanthan gum to increase dissolution rate. *Carbohydr. Polym.* **2003**, *53*, 497−499.

(27) Hong, J.; Kessels, W. M. M.; Soppe, W. J.; Weeber, A. W.; Arnoldbik, W. M.; van de Sanden, M. C. M. Influence of the high-temperature "firing" step on high-rate plasma deposited silicon nitride films used as bulk passivating antireflection coatings on silicon solar cells. *J. Vac. Sci. Technol. B* **2003**, *21*, 2123−2132.

(28) Murthy, S. K.; Olsen, B. D.; Gleason, K. Effect of Filament Temperature on the Chemical Vapor Deposition of Fluorocarbon-Organosilicon Copolymers. *J. Appl. Polym. Sci.* **2004**, *91*, 2176−2185.

(29) Pai, V. B.; Srinivasarao, M.; Khan, S. A. Evolution of microstructure and rheology in mixed polysaccharide systems. *Macromolecules* **2002**, *35*, 1699−1707.

(30) Egelandsdal, B.; Fretheim, K.; Harbitz, O. Dynamic rheological measurements on heat-induced myosin gels: An evaluation of the method's suitability for the filamentous gels. *J. Sci. Food Agric.* **1986**, *37*, 944−954.

Received for review December 10, 2004. Revised manuscript received February 15, 2005. Accepted February 24, 2005.

JF0479113